Glypican-3–deficient Mice Exhibit Developmental Overgrowth and Some of the Abnormalities Typical of Simpson-Golabi-Behmel Syndrome

Danielle F. Cano-Gauci,*‡ Howard H. Song,‡§ Huiling Yang,‡§ Colin McKerlie,§ Barbara Choo,*‡ Wen Shi,‡§ Rose Pullano,*‡ Tino D. Piscione,‖ Silviu Grisaru,‖ Shawn Soon,‖ Larisa Sedlackova,‖ A. Keith Tanswell,‖ Tak W. Mak,*¶ Herman Yeger,‖ Gina A. Lockwood,*‡ Norman D. Rosenblum,‖ and Jorge Filmus‡§

*The Ontario Cancer Institute, Toronto, Ontario, M5G 2M9 Canada; ‡Department of Medical Biophysics, University of Toronto, Toronto, Ontario, Canada; §Sunnybrook Health Science Centre, Toronto, Ontario, M4N 3M5 Canada; ‖Hospital for Sick Children, Toronto, Ontario, M5G 1X8 Canada; and ¶The Amgen Institute, Toronto, Ontario, M5G 2C1 Canada

Abstract. Glypicans are a family of heparan sulfate proteoglycans that are linked to the cell surface through a glycosyl–phosphatidylinositol anchor. One member of this family, *glypican-3* (*Gpc3*), is mutated in patients with the Simpson-Golabi-Behmel syndrome (SGBS). These patients display pre- and postnatal overgrowth, and a varying range of dysmorphisms. The clinical features of SGBS are very similar to the more extensively studied Beckwith-Wiedemann syndrome (BWS). Since BWS has been associated with biallelic expression of insulin-like growth factor II (IGF-II), it has been proposed that GPC3 is a negative regulator of IGF-II. However, there is still no biochemical evidence indicating that GPC3 plays such a role.

Here, we report that GPC3-deficient mice exhibit several of the clinical features observed in SGBS patients, including developmental overgrowth, perinatal death, cystic and dyplastic kidneys, and abnormal lung development. A proportion of the mutant mice also display mandibular hypoplasia and an imperforate vagina. In the particular case of the kidney, we demonstrate that there is an early and persistent developmental abnormality of the ureteric bud/collecting system due to increased proliferation of cells in this tissue element.

The degree of developmental overgrowth of the GPC3-deficient mice is similar to that of mice deficient in IGF receptor type 2 (IGF2R), a well characterized negative regulator of IGF-II. Unlike the IGF2R-deficient mice, however, the levels of IGF-II in GPC3 knockouts are similar to those of the normal littermates.

Key words: glypican-3 • Simpson-Golabi-Behmel syndrome • overgrowth • insulin-like growth factor II • kidney dysplasia

GLYPICANS are a family of heparan sulfate (HS)[1] proteoglycans that are linked to the cell surface through a glycosyl–phosphatidylinositol anchor (David, 1993; Stipp et al., 1994; Filmus et al., 1995; Nakato et al., 1995; Watanabe et al., 1995; Veugelers et al., 1997). The protein cores of glypicans are 20–50% identical. In particular, the location of 13 cysteines and of the consensus sites for the insertion of the HS chains are highly conserved (Saunders et al., 1997). The function of glypicans is still not well understood. Regulatory mutations of *dally* (division abnormally delayed), a *Drosophila* glypican, have a severe impact on the postembryonic development of the nervous system, and generate morphological defects in the eyes, antennae, wings, and genitalia (Nakato et al., 1995). Recently, it has been reported that *dally* controls cellular responses to decapentaplegic, but the molecular basis of this activity is unknown (Jackson et al., 1997). Glypican-1 (GPC1), on the other hand, has the capacity to interact and regulate the activity of fibroblast growth factor-2 and other heparin-binding growth factors in tissue culture (Steinfeld et al., 1996; Bonneh-Barkay et al., 1997; Kleef et al., 1998). The interaction of GPC1 and these

This paper is dedicated to the memory of Ronald N. Buick.

Address all correspondence to Jorge Filmus, Division of Cancer Biology Research, S-218 Research Building, Sunnybrook Health Science Centre, 2075 Bayview Avenue, Toronto, Ontario, M4N 3M5 Canada. Tel.: (416) 480-6100. Fax: (416) 480-5703. E-mail: filmus@srcl.sunnybrook.utoronto.ca

1. *Abbreviations used in this paper:* BrdU, 5 bromo-2′deoxyuridine; BWS, Beckwith-Wiedemann syndrome; DBA, Dolichos biflorus agglutinin; E, embryonic day; ES, embryonic stem; GPC1, glypican-1; GPC3, glypican-3; HS, heparan sulfate; IGF-II, insulin-like growth factor II; IGF2R, IGF receptor type 2; P, postnatal day; SGBS, Simpson-Golabi-Behmel syndrome.

growth factors is mediated by its HS chains, suggesting that GPC1 is regulating the binding of the growth factors to their high affinity receptors (Steinfeld et al., 1996).

Recent work by Pilia et al. (1996) has demonstrated that the *glypican-3* (*Gpc3*) gene is mutated in patients with the Simpson-Golabi-Behmel syndrome (SGBS). This is an X-linked disorder in which patients display pre- and postnatal overgrowth, and a varying range of dysmorphisms that can include a distinct facial appearance, macroglossia, cardiac defects, dysplastic and cystic kidneys, hernias, supernumerary nipples, and various skeletal abnormalities, including polydactyly and syndactyly (Behmel et al., 1984; Neri et al., 1988; Garganta and Bodurtha, 1992; Orstavik et al., 1995; Pilia et al., 1996; Lindsay et al., 1997). Death during infancy is very frequent, usually as a result of pneumonia (Garganta et al., 1992). The clinical features of SGBS suggest that GPC3 is involved in the regulation of cell proliferation and apoptosis during development (Hughes-Benzie et al., 1996). Indeed, we have recently demonstrated that GPC3 can induce apoptosis or inhibit proliferation in a cell-line–specific manner (Dueñas Gonzales et al., 1998; Filmus, J., unpublished observations). It is also important to note that GPC3 is highly expressed during development in the tissues that are affected in SGBS patients (Pellegrini et al., 1998).

SGBS is phenotypically very similar to the more extensively studied Beckwith-Wiedemann syndrome (BWS; Weksberg et al., 1996; Hastie, 1997). Since biallelic expression of the paternally imprinted *insulin-like growth factor-II (Igf2)* gene is thought to play a prominent role in BWS (Brown et al., 1996; Weksberg and Squire, 1996; Sun et al., 1997), it has been proposed that GPC3 is a negative regulator of this growth factor (Pilia et al., 1996). Additional indirect evidence suggesting that GPC3 can act as a negative regulator of IGF-II has been provided recently by the generation of double mutant mice lacking the IGF receptor type 2 (IGF2R), and the *H19* locus (Eggenschwiler et al., 1997). IGF2R is a well characterized negative regulator of IGF-II that binds this growth factor and downregulates its activity by endocytosis and degradation (Ludwig et al., 1996). Meanwhile, the *H19* locus regulates IGF-II imprinting. Consequently, when this locus is deleted, *Igf2* imprinting is suppressed, and biallelic expression is observed (Leighton et al., 1995). As expected, the *Igf2r* and *H19* double mutants display a dramatic increase in circulating and tissue IGF-II levels (Eggenschwiler et al., 1997). In addition, these mice exhibit some of the clinical features of BWS, including developmental overgrowth, visceromegaly, omphalocele, and cardiac, and adrenal defects. Interestingly, skeletal defects that are more typical of SGBS are also observed in these double mutants (Weksberg et al., 1996).

Despite these indirect genetic data suggesting that GPC3 plays a role IGF-II signaling, it is important to note that conclusive biochemical data supporting such a role for GPC3 has not been provided. Therefore, we have generated GPC3-deficient mice in an effort to study SGBS and the molecular basis of its similarity to BWS. We report here that these mice display many of the phenotypic features of SGBS, including developmental overgrowth, perinatal death, abnormal lung development, and cystic kidneys. Developmental overgrowth, however, was not accompanied by higher levels of circulating IGF-II or by a significantly increased expression of this growth factor in tissues.

Materials and Methods

Targeting Vector

A 6.5-kb portion of the *Gpc3* gene was cloned by screening a 129J-1 Dash II genomic library with the 5′ end of the *Gpc3* cDNA. A SmaI fragment within the 6.5-kb genomic clone that included part of the promoter region and exon 1 was replaced by an EcoRI/BglII fragment containing the neomycin-resistance gene under the control of the PGK promoter, driving expression in the antisense direction (neo cassette). The final targeting vector carried the PGK–neo cassette flanked by part of the *Gpc3* promoter and the first intron at the 5′ and 3′ ends, respectively (Fig. 1 A). The vector was linearized and used to electroporate 129/J embryonic stem (ES) cells. Transfected clones resistant to G418 were screened by PCR for homologous recombination. Two recombinant ES clones, 8D1 and 7F12, were then used for injections into C57BL/6 blastocysts. Germline transmission was identified by Southern blot analysis of EcoRI-digested genomic DNA using a SmaI/KpnI fragment (S1) of the genomic clone. Mice were subsequently genotyped using PCR as follows: the presence of the neo cassette was determined by amplifying a neo-specific band using primers PCR2 and neo, followed by primers PCRL2 and neo in nested PCR reactions; a single denaturation step (95°C for 5 min) was followed by 25 cycles (94°C for 2 min, 55°C for 2 min, and 72°C for 3 min), with a final single elongation step (72°C for 5 min). To detect the 420-bp wild-type fragment of the *Gpc3* gene to distinguish heterozygous and homozygous mutants, primers PCRL3 and PCR5 were used in 25 cycles (94°C for 30 s, 55°C for 30 s, and 72°C for 30 s), followed by a final elongation step (72°C for 5 min). Primers were: PCR2, 5′-GTGTGGTTCTATTGAATGGACCC-3′; neo, 5′-GCCAGCTCATTCCTCCACTCAT-3′; PCRL2, 5′-ACGTGACTATTTGTGGGTAGG-3′; PCRL2, 5′-ACGTGACTATTTGTGGGTAGG-3′; PCRL3, 5′-TTGCCACTCTCTCGTGCTCTCC-3′; and PCR5, 5′-CAGAGTCCATACTGTGCTTCC-3′.

Measurement of Embryonic Growth

For staging embryos, noon of the day of a vaginal plug was considered E0.5. For weighing, embryos were dissected out of their yolk sacs and patted dry.

Measurements of IGF-II Levels

The quantification of IGF-II by Western blot was performed according to a previously published method (Ludwig et al., 1996). In brief, embryos were homogenized in 1 M acetic acid and incubated for 1 h in ice. Homogenates were then spun at 15,000 rpm for 10 min and supernatants were neutralized with 5 N NaOH. After spinning again at 15,000 rpm for 10 min, proteins were precipitated from the supernatant with trichloroacetic acid (final concentration 20% vol/vol). Pellets were washed twice with 80% ethanol/100 mM Tris, pH 7.5, and were solubilized in SDS-PAGE loading buffer. Protein concentration was determined using the BCA reagent (Pierce Chemical Co.). Typically, 20–50 μg of protein or 16 μl of serum (previously diluted 1:3 with 1% SDS) were run on a 10–20% SDS-PAGE gradient gel. Equal protein loading was confirmed by Coomassie blue staining. Proteins were transferred to a PVDF membrane in a 10 mM CAPS buffer, pH 11.0. Membranes were then incubated with 0.1 μg/ml of an anti-rat IGF-II antibody (Amano) followed by an anti-mouse streptavidin-conjugated secondary antibody (Sigma Chemical Co.). Bound antibody was visualized using Biotin-HRP and chemiluminescence. The intensity of the bands corresponding to IGF-II was measured with a scanning densitometer (Molecular Dynamics, Inc.) and compared with the intensity of bands corresponding to different amounts of recombinant IGF-II.

For Northern blot analysis, tissue extracts were prepared using a Polytron. RNA was extracted using trizol (GIBCO BRL). After electrophoretic separation and transfer to a membrane, the RNA was probed with mouse *Igf2* cDNA. To correct for equal loading, the membrane was stripped and reprobed with a GAPDH cDNA. The intensity of the bands corresponding to IGF-II and GAPDH was measured with a scanning densitometer.

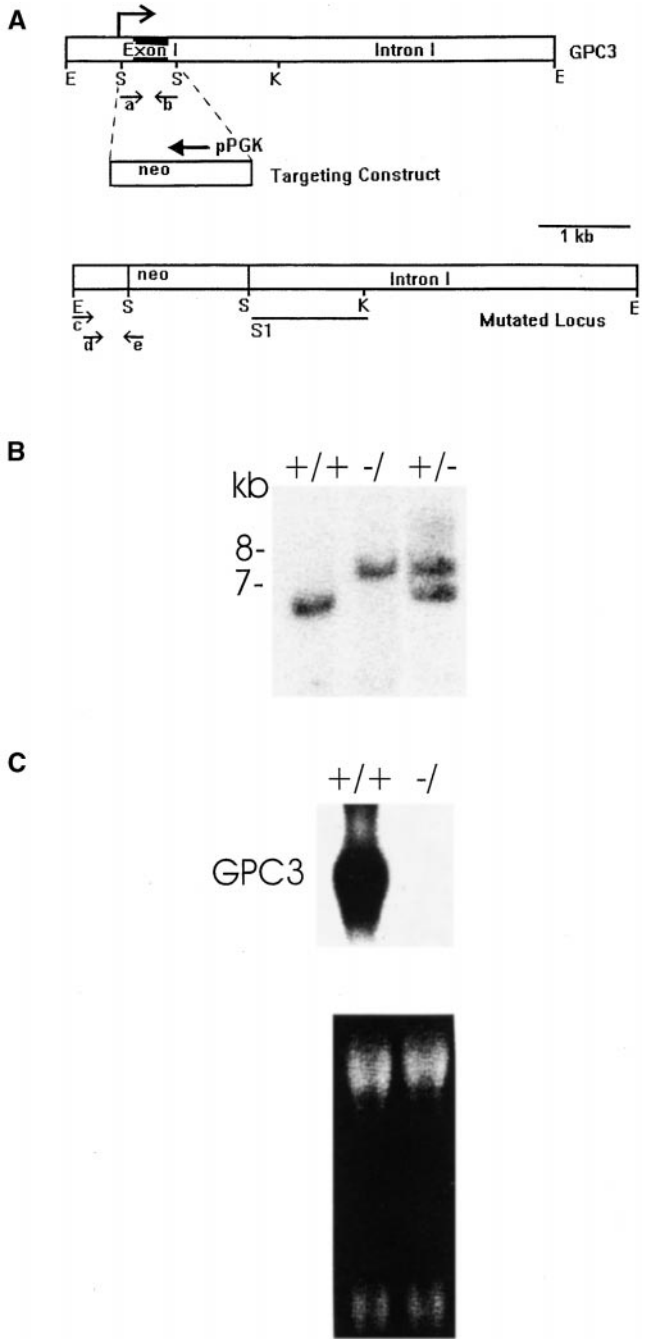

Figure 1. Gene targeting of the murine *Gpc3* locus. (A) A 6.5-kb EcoRI fragment of the murine *Gpc3* locus is shown (top). The SmaI fragment containing the promoter, the transcription start site (arrow), exon 1, and part of intron 1 is indicated. An EcoRI/Bg1II fragment containing the neo cassette, a neomycin gene with a PGK promoter, driving expression in the antisense direction, is shown in the middle. The mutated locus with the neo cassette replacing the SmaI fragment is shown below. Restriction enzyme sites are as follows: E, EcoRI; K, KpnI; S, SmaI. The probe (S1) hybridized to the 6.5-kb wild-type and 7.5-kb targeted allele fragments, as expected. PCR primer sites and orientation within the native and disrupted loci are indicated: a, PCRL3; b, PCR5; c, PCR2; d, PCRL2; and e, neo. (B) Southern blot analysis of EcoRI-digested genomic DNA extracted from tail biopsies of wild-type, heterozygous, and hemizygous mutant offspring (+/+, +/−, and −/, respectively). (C) Top, Northern blot analysis of GPC3 in wild-type (+/+) and (−/) E18.5 embryos. 10 μg total RNA was probed with a 2.2-kb full-length *Gpc3* cDNA. Bottom, ethidium bromide staining demonstrates equal loading.

Histopathology

Whole embryos, excised organs, or pups that had been subjected to a midline incision were fixed in 10% neutral buffered formalin at room temperature overnight before paraffin embedding using standard histological techniques. Paraffin blocks were sectioned at 5–6 μm and stained with hematoxylin and eosin. Embryonic skeletons were stained with Alcian blue and Alizarin red S (Bullock et al., 1998).

Cell Proliferation and Apoptosis in Embryonic Kidney

Pregnant mice were injected intraperitoneally with 5 bromo-2′deoxyuridine (BrdU) 100 μg/g body weight. Embryos were surgically removed 3 h later and kidneys were isolated and fixed in 4% formaldehyde in PBS, pH 7.4. Paraffin-embedded kidney tissue sections were deparaffinized in xylene, rehydrated in a graded ethanol series, rinsed in PBS, and then either processed further for BrdU staining or stained directly with hematoxylin and eosin. Sections used for BrdU assays were treated with trypsin for 5 min at 37°C and then processed for BrdU detection using commercially available reagents (Boehringer Mannheim). To identify ureteric buds/collecting ducts, sections were stained for 1 h at room temperature with Dolichos Biflorus agglutinin (DBA; Vector Labs, Inc.) diluted 1:100 in blocking buffer consisting of 5% goat serum (Life Technologies, Inc.), 3% BSA (ICN Biochemicals), and 0.01% Tween 20 (Sigma Chemical Co.) in PBS, pH 7.4. Sections were then dehydrated in a graded ethanol series, treated with xylene for 10 min, and mounted with DPX Mountant (VWR Scientific).

BrdU-labeled E13 kidney tissue sections were imaged sequentially at 400× by bright-field and fluorescence microscopy using an Axioskop microscope (Carl Zeiss) fitted with an HBO 50 W vapor short-arc lamp using a Shott 38 band-pass filter and a 3-FL fluorescence reflector. Entire sections of renal tissue were reconstructed on the benchtop by building a composite from the photographed images. The composite was analyzed by counting the proportion of BrdU-labeled cells within the population of ureteric bud/collecting duct cells (DBA positive) and mesenchymal cells (DBA negative).

Results

Generation of GPC3-deficient Mice

To generate GPC3-deficient mice by homologous recombination, a targeting construct designed to remove part of the promoter region and the first exon of *Gpc3* (Fig. 1 A) was transfected into 129/J ES cells. Several clones that displayed homologous recombination were then injected into C57BL/6 blastocysts. Since *Gpc3* is X-linked, the backcrossing of F1 heterozygous females with wild-type C57BL/6 males was expected to generate male null mutants (−/). Indeed, that was the case, as shown by Southern blot analysis (Fig. 1 B). The lack of expression of GPC3 in the −/ mice was confirmed by Northern blot (Fig. 1 C). 226 F2 backcross mice were typed by PCR and 47 (21%) were found to be −/. This is close to the 25% predicted by Mendelian inheritance, and evidence of embryonic lethality was not found. However, 10 of the 47 *Gpc3* −/ mice died before weaning. After successive backcrossing to C57BL/6, it became evident that the lack of GPC3 expression increasingly affected viability. For example, after the fourth backcross (N4), only 21 (10%) of the mice that could be typed (many were cannibalized) were hemizygous mutants, and only two out of these 21 mice survived to weaning. Similar perinatal lethality was observed when the backcrossing was performed with Balb/c mice (data not shown). By the eighth backcross (N8) in the C57BL/6 strain (almost congenic), all mice died perinatally. These results indicate that the phenotype of *Gpc3* −/ mice is highly dependent on the genetic background. Unless otherwise indicated, all studies described were performed in

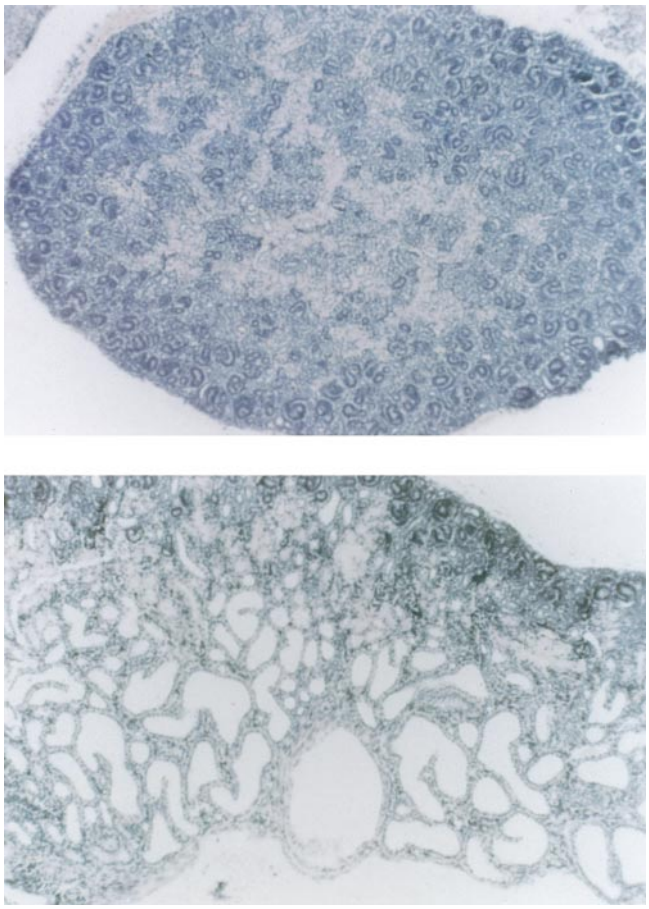

Figure 2. Histological analysis of kidney sections. Kidney sections from 4-d-old wild-type (top) and GPC3-deficient (bottom) littermates were fixed and sections stained with hematoxylin and eosin.

mice obtained from backcrosses 7 to 9 (N7 to N9) with the C57BL/6 strain.

Anatomical examination of mice from N4 and successive backcrosses revealed the presence of cystic and dysplastic kidneys in all *Gpc3* −/ and some female *Gpc3* +/− mice (Fig. 2). These abnormalities were seen in a large proportion of mice from earlier backcrosses, also. However, the degree of dysplasia varied significantly from mouse to mouse.

As discussed above, a proportion of *Gpc3* −/ mice survived beyond the first day, particularly in earlier backcrosses (N2 to N4). Many of these mice, however, died before weaning. Histological analysis revealed the presence of bacterial infection in the respiratory tract (pneumonia and rhinitis), as well as an accumulation of cellular debris and mucus in small and medium size bronchioles. Although there were no obvious differences between wild-type and mutant mice at E18 (embryonic day 18; Fig. 3), as early as P0 (postnatal day 0) the lumens of airways contained an admixture of stranding mucus and sloughed epithelial cells. By P5, the amount of mucus had increased and was distributed over the entire surface of the respiratory epithelium. These lesions may have contributed to the perinatal death and increased susceptibility of *Gpc3* −/ mice to respiratory infections.

In our initial examination of the newborn *Gpc3* −/ mice, no obvious skeletal abnormalities were observed by X-ray analysis or staining. However, when mutant embryos from backcrosses N7 and N8 were examined, a proportion of them (10%) were found to have severe mandibular hypoplasia (Fig. 4). Histological analysis of jaw sections revealed no bone constituting the rami of the mandible, which consisted only of myxomatous stroma with overlying haired skin (data not shown).

To generate female *Gpc3* −/− mice, the few *Gpc3* −/ mice that reached adulthood in the early backcrosses were mated with *Gpc3* +/− mice. The *Gpc3* −/− female mice generated in this way displayed a phenotype similar to the *Gpc3* −/ mice. In addition, mutant females had an imperforate vagina with higher frequency (30%) than is found in the normal population (4%; Cunliffe-Beamer and Feldman, 1976). As a consequence, these mice experienced marked swelling of the perineum and the uterus was fluid-filled, such that it was several times its normal size.

Developmental Overgrowth of Gpc3 −/ Mice

To determine if GPC3-deficient mice exhibit overgrowth, as SGBS patients do, we compared the weight of *Gpc3* −/, +/−, and +/+ littermates at different stages of embryonic development. Fig. 5 shows that the *Gpc3* −/ mice were significantly heavier than the wild-type littermates at every time point analyzed. The overgrowth was greater at the time of birth, when the GPC3-deficient mice were ~30% heavier than normal littermates. Heterozygotes displayed an intermediate size at all time points. When we compared heart, lung, and liver weight as percentage of body weight at different embryonic stages, we found no significant differences between *Gpc3* +/+ and −/ mice. Lungs from *Gpc3* −/ mice, however, were disproportionally heavy at time of birth, weighing 28% more than their normal littermates (data not shown). Since this disproportionate overgrowth is only evident in newborn mice, we speculate that it is due to the accumulation of debris observed in the lungs after birth (Fig. 3). With regard to the kidneys, while those from E13.5 −/ embryos were disproportionally larger than kidneys from the normal littermates (see Fig. 7), comparison of weight at E16.5, E18.5, and P0 did not show a statistically significant disproportionate overgrowth. This may be explained by the observation that the medulla of the −/ kidneys begins to degenerate by E15.5, resulting in a reduction in whole kidney mass.

Currently, the molecular basis by which GPC3 regulates growth is unknown. Based on the phenotypic overlap between SGBS and BWS, and the fact that biallelic expression of IGF-II has been associated with BWS, it has been proposed that GPC3 is a negative regulator of IGF-II (Pilia et al., 1996). Interestingly, developmental overgrowth of a similar magnitude to that observed in GPC3-deficient mice has been reported in IGF2R-deficient mice (Lau et al., 1994; Wang et al., 1994). These mice have increased levels of circulating (about fourfold) and tissue (about twofold) IGF-II (Lau et al., 1994). This is not surprising, since this receptor binds IGF-II and downregulates its activity by endocytosis and degradation. Thus,

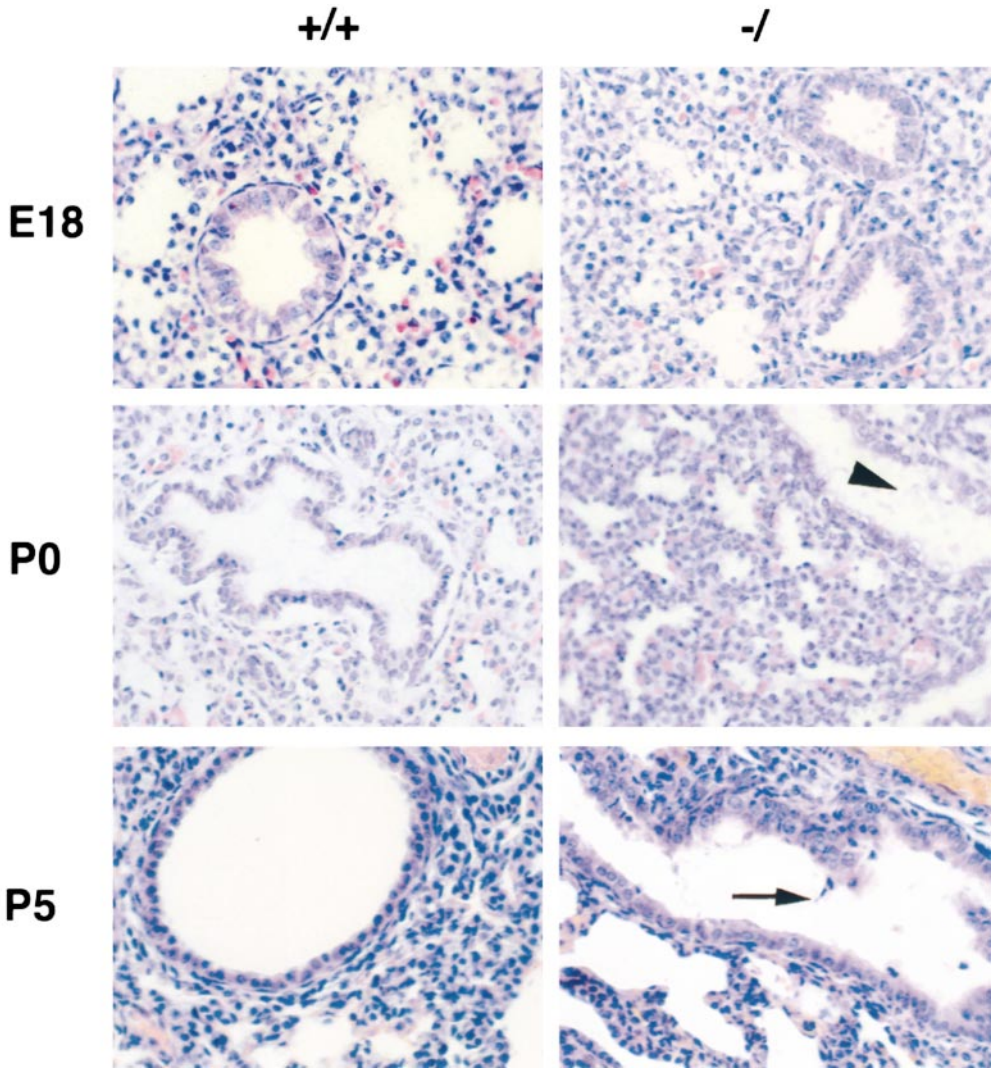

Figure 3. Histological analysis of wild-type (+/+) and GPC3 deficient (−/) lungs. Hematoxylin and eosin stained sections of lungs at E18, P0, and P5 are shown. Accumulation of mucus (arrowhead) and cellular debris (arrow) is indicated. Original magnification is 400.

to investigate whether the overgrowth observed in the GPC3-deficient mice could also be due to increased levels of IGF-II, we measured its serum and tissue levels in wild-type and *Gpc3*-mutant mice. As shown in Fig. 6 A, the mutant mice show no significant differences in circulating IGF-II levels compared with wild-type at developmental stages in which overgrowth in the GPC3-deficient mice was documented. We also compared the levels of IGF-II in protein extracts of whole embryos at E12.5 and E14.5. As shown in Fig. 6, IGF-II levels were similar in *Gpc3* −/ embryos and their normal littermates. Since the levels of mature IGF-II in embryonic liver, lung, and kidney are too low to be measured accurately by Western blot, we assessed the levels of IGF-II mRNA in liver, lung, and kidney of E18 embryos by Northern blot. No significant difference could be detected between *Gpc3* −/ and normal littermates (Fig. 6).

GPC3 Regulates Cell Proliferation in the Developing Renal Collecting System

To identify abnormalities that underlie the renal cysts and dysplasia of *Gpc3* −/ mice, embryonic kidneys from N5 to N8 mice were studied. The E12 normal kidney is characterized by invasion of the blastema by the ureteric bud, formation of a T-shaped branched ureteric bud, and condensation of the blastemal cells around the invading ureteric bud (Sorokin and Ekblom, 1992; Fig. 7). Compared with their normal littermates, E12 −/ kidneys displayed a larger number of ureteric bud branches (Fig. 7). Development of the blastemal compartment in these kidneys was consistent with the enhanced development of the ureteric bud component. Quantification of the mass of ureteric bud, identified by DBA staining in tissue sections using digitized images, indicated a threefold increase of ureteric bud surface area in hemizygous null kidneys compared with wild-type (7,063 ± 108 versus 2,380 ± 230 arbitrary units, $P < 0.03$, two separate litters).

E13.5 *Gpc3* −/ kidneys displayed similar abnormalities to that of E12 kidneys. In addition, they looked significantly larger than the kidneys from the normal littermates (Fig. 7). By E16.5, disruption of tissue development was evident in the *Gpc3* −/ kidneys. While normal looking cortical tissue elements (glomeruli and tubules) were present

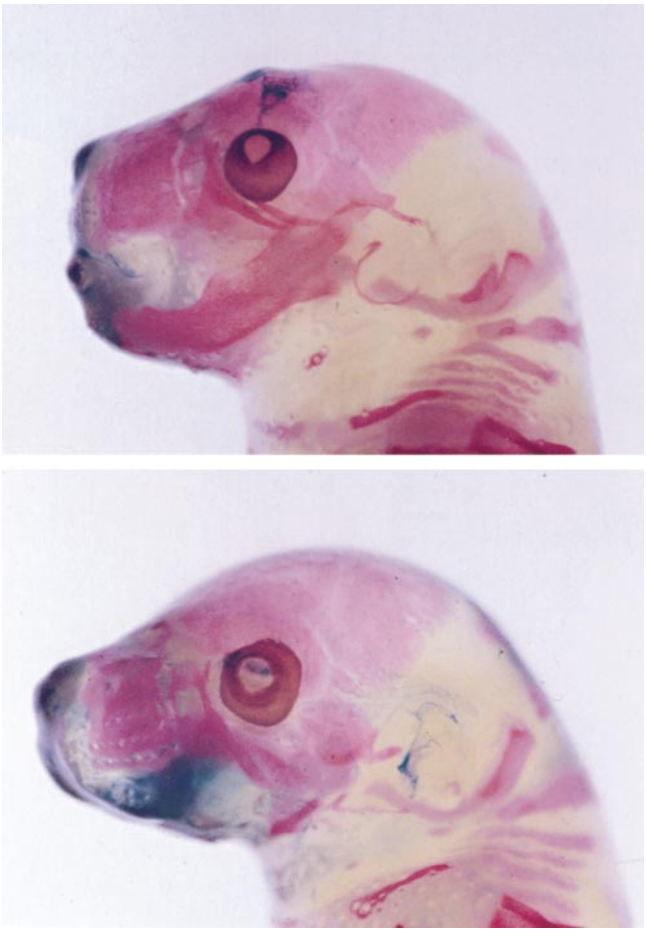

Figure 4. Mandibular hypoplasia in *Gpc3* −/ embryos. Alizarin red/Alcian blue skeletal preparations of wild-type (top) and *Gpc3* −/ (bottom) E18.5 embryonic heads are shown. Note the complete lack of mandible in the mutant embryo.

in mutant kidneys, the organization of these elements was abnormal compared with wild-type. In addition, the tubular mass in the medulla was reduced. This was accompanied by formation of epithelial cysts (Fig. 7). By E18.5, the dysplastic appearance of the medulla was fully evident. Whereas a compact and highly patterned network of tubules was present in the wild-type kidney, the medullary tubules in *Gpc3* −/ kidneys were decreased in number, disorganized, and often cystic (Fig. 7).

We hypothesized that a disregulation of cell proliferation might underlie the accelerated ureteric bud development observed in *Gpc3* −/ kidneys. Thus, cell proliferation in the ureteric buds/collecting ducts was assessed by measuring BrdU incorporation into DNA. Quantification of BrdU uptake in four sets of wild-type and *Gpc3* −/ mice at E12.5 demonstrated a 2.8-fold increase in the percentage of cells that incorporated BrdU in the epithelial cells of the collecting system, identified by DBA binding (Fig. 8 A). This enhancement of BrdU uptake in the collecting system persisted at E13.5 (2.6-fold increase) and E16.5 (3.4-fold increase). In contrast, while the basal rate of cell proliferation was generally high in mesenchymal cells adjacent to the collecting system (identified by morphology and lack of staining with DBA), there was no significant difference in mesenchymal cell proliferation in the kidneys of *Gpc3* +/+ versus *Gpc3* −/ mice at E 12.5 (27.6 ± 3.0% versus 30.0 ± 1.7%), E13.5 (18.7 ± 3.0% versus 24.0 ± 1.7%), or E16.5 (21.2 ± 2.7% versus 24.3 ± 6.4%; four independent samples, 250 mesenchymal cells counted per sample).

Taken together, the analysis of cell proliferation in developing kidneys of *Gpc3* −/ mice indicates an early and persistent abnormality in ureteric bud development due to increased proliferation of cells intrinsic to this tissue element. This observation provides an eloquent example of the critical role of GPC3 in the regulation of developmental growth.

Discussion

We report in this paper that GPC3-deficient mice exhibit several of the clinical features of SGBS patients, including developmental overgrowth, perinatal death, cystic and dysplastic kidneys, and abnormal lung development. Other abnormalities observed in some SGBS patients, such as hernias, heart defects, polydactyly, and vertebral and rib malformations, are not present in the mutant mice. Conversely, GPC3-deficient mice display mandibular hypoplasia and an imperforate vagina, two clinical features that have not been described in SGBS patients. It is interesting to note that an imperforate vagina could be the result of deficient apoptosis of the vaginal epithelial cells during sexual maturation (Jacobson et al., 1997). This is consistent with our recent finding that GPC3 can induce apoptosis in certain cell types (Dueñas Gonzalez et al., 1998).

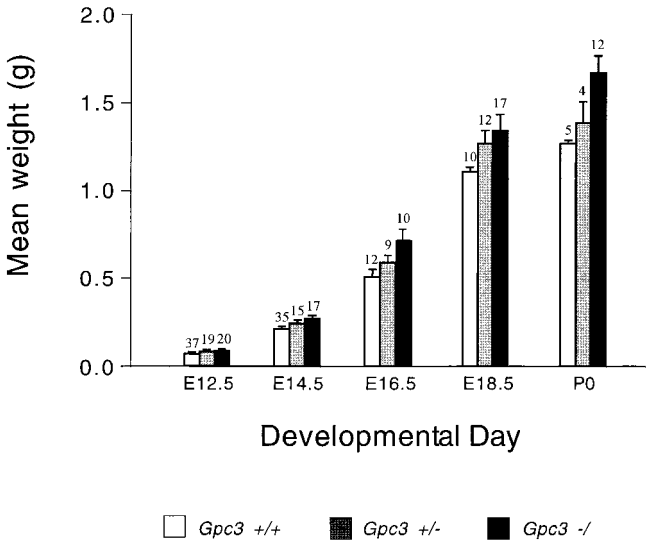

Figure 5. Embryonic growth kinetics. Wild-type, heterozygous, and knockout embryos were weighed at the indicated embryonic day and at birth. Bars represent the average embryo wt + 2 SEM. Total number of embryos weighed for each group is indicated above each bar. Statistical analysis using a *t* test showed significant differences ($P < 0.05$) between mean weight of the three genotypes at each time point analyzed, with the exception of wild-type and heterozygous at P0, and heterozygous and knockout at E12.5 and E18.5.

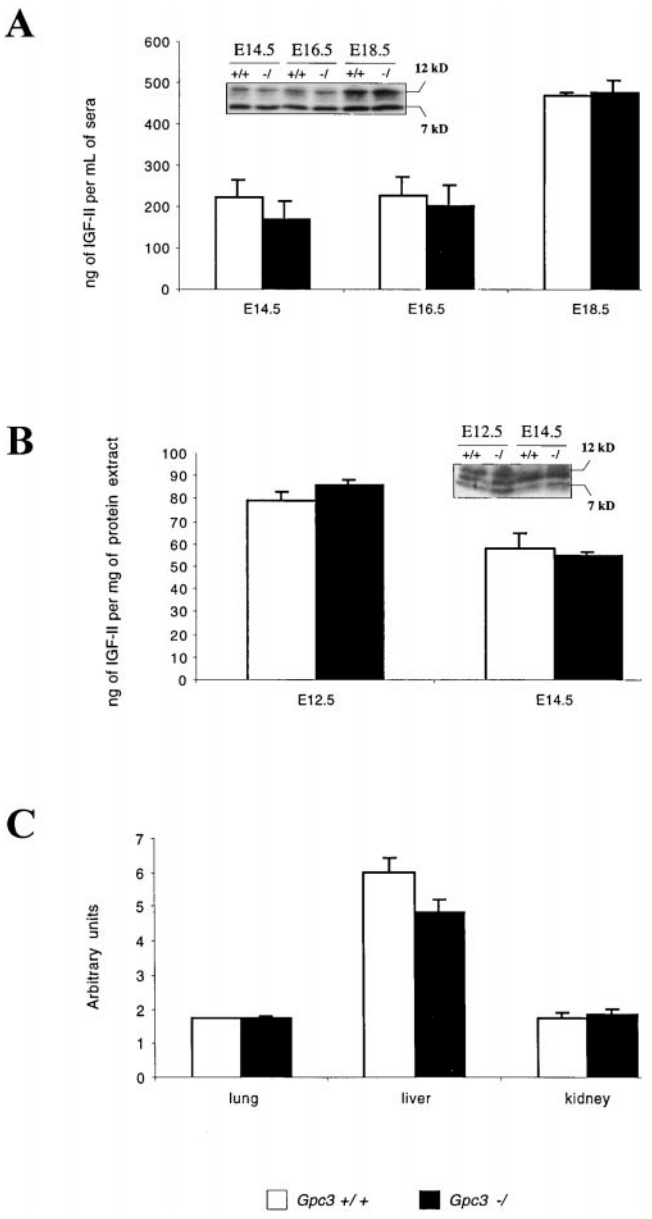

Figure 6. Comparative analysis of IGF-II levels in serum, whole embryo, lung, liver, and kidney. (A) Circulating levels of IGF-II at different time points during development. (B) Levels of IGF-II in whole embryos at E12.5 and E14.5. Each bar represents the mean + SEM obtained by densitometric scanning of four pooled samples done in duplicate. Inset shows a representative image of the Western blot. (C) IGF-II mRNA levels were measured by Northern blot analysis and normalized with the intensity of the corresponding GAPDH band. Each bar represents the mean + SEM obtained by densitometric scanning of two different samples.

Although not all the clinical features observed in SGBS patients are found in the GPC3-deficient mice, we consider that there are enough similarities to justify the use of these mice as a model to study SGBS. In particular, these mice will be useful to study the role of GPC3 in the regulation of growth during development. Indeed, we are reporting here that *Gpc3* −/ mice display hyperplasia of the developing ureteric bud/collecting duct system. Most likely this hyperplasia explains, at least in part, the cystic and dysplastic phenotype of the kidneys in the GPC3-deficient mice and SGBS patients. In addition, the GPC3-deficient mice will be useful to study the role of GPC3 in lung development. In this respect, it is interesting to note that SGBS patients, like the *Gpc3* −/ mice, also develop respiratory infections with high frequency (Garganta and Bodurtha, 1992).

The similarities between SGBS and BWS have suggested the hypothesis that GPC3 regulates IGF-II activity. Furthermore, the IGF2R-deficient mice display a degree of developmental overgrowth similar to the *Gpc3* −/ mice. In contrast to the *IGF2R* knockouts, however, the GPC3-deficient mice do not show any increase in circulating or local expression of IGF-II (Fig. 6). Moreover, we have been unable to detect direct interaction between GPC3 and IGF-II (Song et al., 1997). It can be concluded, therefore, that if GPC3 inhibits IGF-II signaling, it does so by a mechanism that is fundamentally different than the one used by the IGF2R.

Eggenschwiler et al. (1997) have recently generated double mutant mice that exhibit a dramatic increase in circulating and tissue IGF-II. These investigators have proposed that, in addition to the clinical features of BWS, these mice display skeletal abnormalities typical of SGBS (Table I). However, SGBS patients and GPC3-deficient mice display severe renal abnormalities, and no such abnormalities have been found in the double mutant mice, despite the fact that they express extremely high levels of IGF-II. Moreover, none of the other mice models that overexpress IGF-II (*Igf-II* transgenics and *Igf2R* knockouts) display any renal alterations. Thus, it is reasonable to propose that even if GPC3 is able to regulate IGF-II signaling, it may have other functions in addition to IGF-II regulation. In this regard, we have shown that GPC3 can bind fibroblast growth factor-2 (Song et al., 1997), and others have demonstrated that GPC1 can regulate the response of several cell types to heparin-binding growth factors (Steinfeld et al., 1996; Kleef et al., 1998). Since these interactions are mediated by the glypicans' HS chains, it is possible that GPC3 interacts with other factors that are known to bind to HS, including members of the transforming growth factor-β and Wnt families. Interestingly, some members of these families are known to play a role in kidney development (Vainio and Muller, 1997; Woolf and Cale, 1997).

Recently, it has been reported that ∼5% of BWS patients show germline mutations of p57, a cyclin-dependent kinase inhibitor (Hatada et al., 1996). In addition, it has been suggested that p57 can also be silenced at the transcriptional level in BWS patients without germline mutations (Lee et al., 1999). Interestingly, p57-deficient mice show kidney dysplasia, adrenal cytomegaly, and omphalocele, but not overgrowth or other features of BWS patients (Zhang et al., 1997; Table I). Since mice overexpressing IGF-II, unlike p57-deficient mice, do not show renal abnormalities, it has been proposed that suppression of p57 expression is a key contributor to the phenotype of BWS patients (Hastie, 1997). This raises the question as to whether p57 could be mediating some of the signals regulated by GPC3, and this issue should certainly be the subject of future investigations.

Given the complexity and heterogeneity of the pheno-

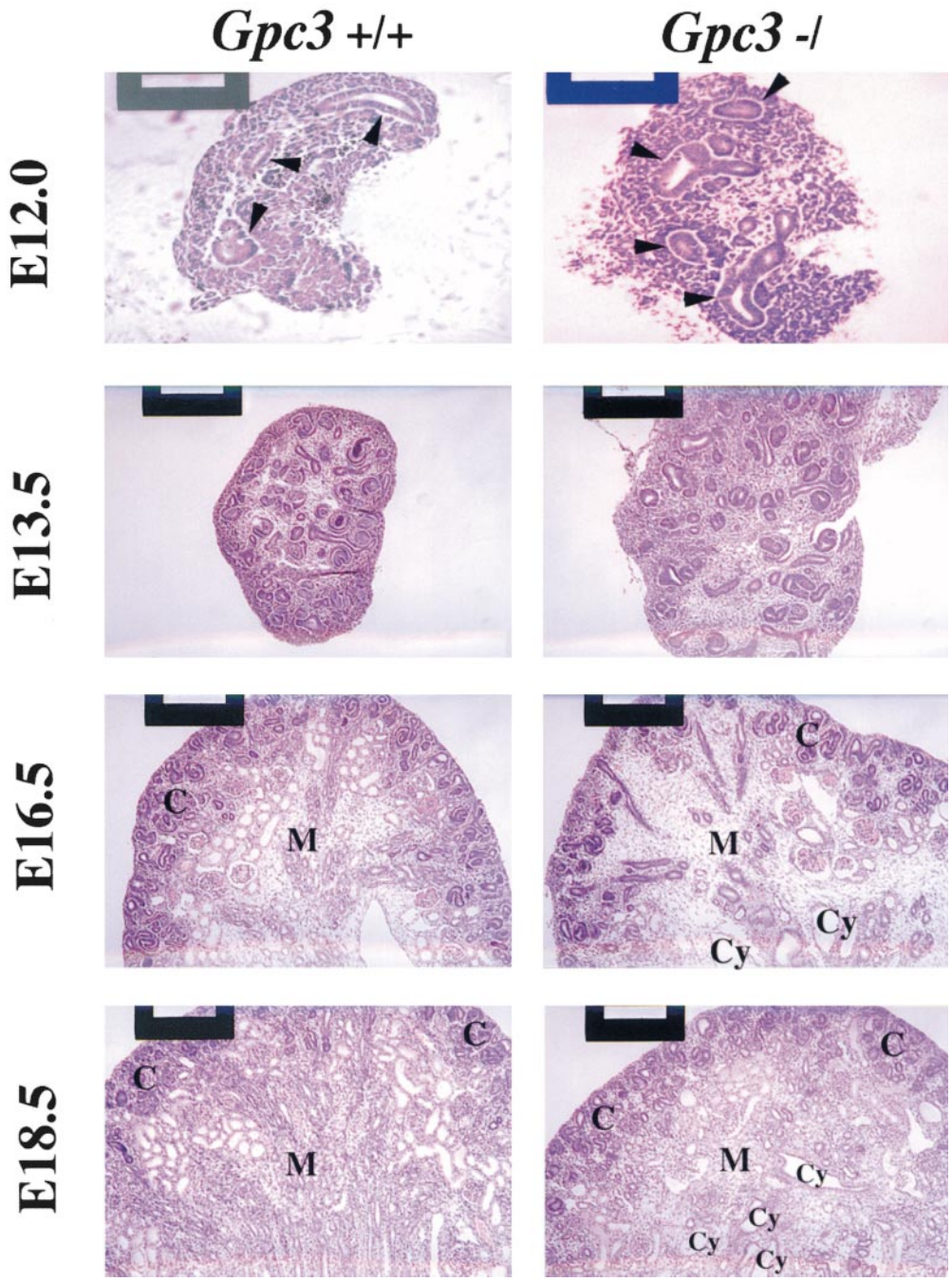

Figure 7. Kidney development in the *Gpc3* −/ mouse. Paraffin-embedded tissue sections were generated from fixed tissue isolated from +/+ and −/ mice. E12.0 sections were imaged at 200×. Bar, 37.5 μm. E13.5, E16.5, and E18.5 sections were imaged at 100×. Bar, 75 μm. At E12.0, branching of the ureteric bud is markedly enhanced in the −/ versus +/+ embryo (arrowheads). By E13.5, the −/ kidney is much larger than that of its +/+ littermate and consists of histologically normal ureteric bud and mesenchymal-derived tissue elements. While these mesenchymal-derived elements (glomeruli and tubules) are present in the cortex (C) of the E16.5 −/ and +/+ kidneys, they are disorganized in the −/ cortex and the −/ medulla (M) is relatively devoid of tubular structures. Cysts (Cy) are present in −/ medulla in an irregular pattern. At E18.5, these abnormalities persist in the −/ kidney and are accompanied by total absence of the medullary tubular patterning characteristic of the +/+ kidney.

Table I. Comparison of Phenotypes

	SGBS	BWS	IGF2R−/−	IGF-II overexpressing	p57−/−	GPC3−/
Overgrowth	+	+	+	+	−	+
Increased circulating IGF-II	ND	ND	+	−	ND	−
Perinatal death	+/−	+/−	+	+	+	+
Kidney dysplasia	+/−	+/−	−	−	+	+
Cardiac defects	+/−	−*	+	+	−	−
Lung abnormalities/infection	+/−	−	+/−	−	−	+
Polydactyly	+/−	−	+	+	−	−
Cleft palate	+/−	−*	−	+	+	−
Vertebral abnormalities	+/−	−	+	+	−	−
Endochondral bone ossification defects	−	−	−	−	+	−
Macroglossia	+/−	+	−	+/−	−	−
Omphalocele	−	+	−	+	+/−	−
Umbilical hernia	+/−	+/−	−	ND	+	−
Adrenal cysts	−	+	−	+	−	−
Adrenal cytomegaly	−	+	−	−	+	−

+, Observed commonly; +/−, less commonly observed; −*, rarely observed; −, not seen at all; ND, not studied. Data were extracted from the following original reports or reviews: Garganta et al., 1992; Lau et al., 1994; Wang et al., 1994; Weng et al., 1995; Hughes-Benzie et al., 1996; Ludwig et al., 1996; Eggenschwiler et al., 1997; Yan et al., 1997; Zhang et al., 1997; Neri et al., 1998.

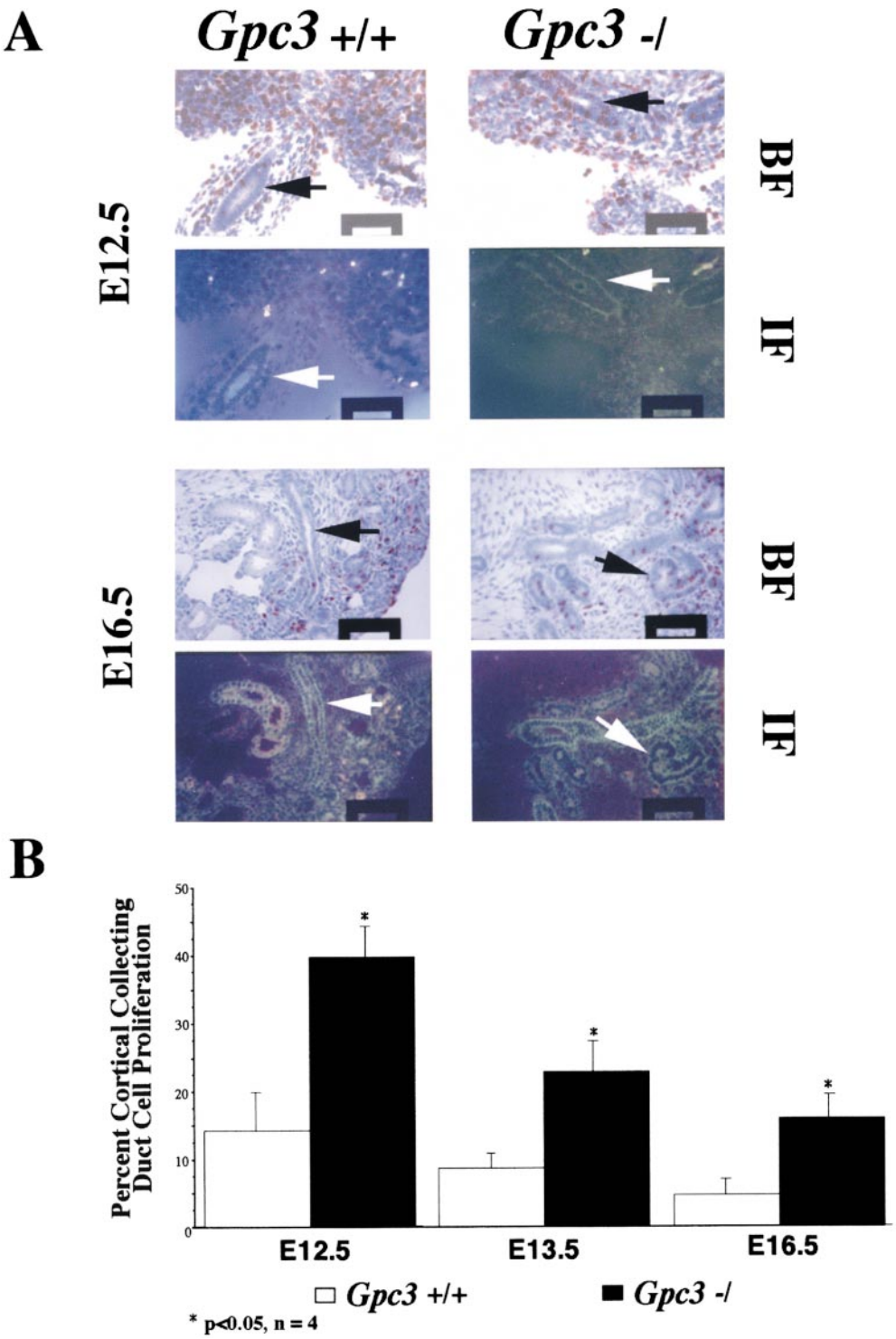

Figure 8. Analysis of cell proliferation in the renal collecting system of the GPC3-deficient mice. Incorporation of BrdU into cells of the ureteric buds or collecting ducts, identified by fluorescein-conjugated DBA, was detected in tissue sections of embryonic kidneys using an anti-BrdU peroxidase-conjugated antibody. (A) Bright-field (BF) and fluorescence (IF) images of representative kidney sections from *Gpc3* +/+ and *Gpc3* −/ mice at E12.5 and E16.5. The arrows mark the position of typical ureteric buds or collecting ducts, identified by fluorescein-DBA. BrdU-labeled cells (brown) are present in both the collecting system and in tissue elements derived from the metanephric blastema, and are more numerous in the cells of the collecting system of the *Gpc3* −/ mice. Bar, 18.7 μm (400×). (B) Quantification of cell proliferation in the ureteric buds or collecting ducts in the kidneys of *Gpc3* +/+ and *Gpc3* −/ mice at E12.5, E13.5, and E16.5. Percent proliferation was calculated as the ratio of BrdU-labeled cells to the total number of ureteric bud or collecting duct cells analyzed. Bars represent the mean + SEM.

typic features of SGBS and BWS, we consider it unlikely that the role of the molecules suspected to be involved in the generation of these disorders will be resolved simply by genetic manipulation of mice (see Table I). It is evident that biochemical studies will be required to clarify the connection between the different molecules involved.

We thank Cassandra Cheng for secretarial assistance and Madeline Li, Andrew Wakeham, and Arda Shahinian for help with animal husbandry and ES cell culture.

This work was supported by grants from the Medical Research Council of Canada and the National Cancer Institute of Canada to J. Filmus, and a Sunnybrook Trust for Medical Research to C. McKerlie. T. Piscione is a fellow of the Kidney Foundation of Canada. S. Grisaru was supported by the Hospital for Sick Children Training Center.

Submitted: 16 April 1999
Revised: 1 June 1999
Accepted: 7 June 1999

References

Behmel, A., E. Plochl, and W. Rosenkranz. 1984. A new X-linked dysplasia gigantism syndrome: identical with the Simpson dysplasia syndrome? *Hum. Genet.* 67:409–413.

Bonneh-Barkay, D., M. Shlissel, B. Berman, E. Shaoul, A. Admon, I. Vlodavsky, D.J. Carey, V.K. Asundi, R. Reich-Slotky, and D. Ron. 1997. Identification of glypican as a dual modulator of the biological activity of fibroblast growth factors. *J. Biol. Chem.* 272:12415–12421.

Brown, K.W., A.J. Villar, W. Bickmore, J. Clayton-Smith, D. Catchpoole, E.R. Maher, and W. Reik. 1996. Imprinting mutation in the Beckwith-Wiedemann syndrome leads to biallelic IGF2 expression through an H19-independent pathway. *Hum. Mol. Genet.* 5:2027–2032.

Bullock, S.L., J.M. Fletcher, R.S.P. Beddington, and V.A. Wilson. 1998. Renal agenesis in mice homozygous for a gene trap mutation in the gene encoding heparan sulfate 2-sulfotransferase. *Genes Dev.* 12:1894–1906.

Cunliffe-Beamer, T.L., and D.B. Feldman. 1976. Vaginal septa in mice: incidence, inheritance, and effect on reproductive performance. *Lab. Anim. Sci.* 26:895–898.

David, G. 1993. Integral membrane heparan sulfate proteoglycans. *FASEB J.* 7:1023–1030.

Dueñas Gonzalez, A., M. Kaya, W. Shi, H. Song, J.R. Testa, L.Z. Penn, and J. Filmus. 1998. OCI-5/GPC3, a glypican encoded by a gene that is mutated in the Simpson-Golabi-Behmel overgrowth syndrome, induces apoptosis in a cell line-specific manner. *J. Cell Biol.* 141:1407–1414.

Eggenschwiler, J., T. Ludwig, P. Fisher, P.A. Leighton, S.M. Tilghman, and A. Efstratiadis. 1997. Mouse mutant embryos overexpressing IGF-II exhibit phenotypic features of the Beckwith-Wiedemann and Simpson-Golabi-Behmel syndromes. *Genes Dev.* 11:3128–3142.

Filmus, J., W. Shi, Z.M. Wong, and M.J. Wong. 1995. Identification of a new membrane-bound heparan sulfate proteoglycan. *Biochem. J.* 311:561–565.

Garganta, C.L., and J.N. Bodurtha. 1992. Report of another family with Simpson-Golabi-Behmel syndrome and a review of the literature. *Am. J. Med. Genet.* 44:129–135.

Hastie, N. 1997. Disomy and disease resolved? *Nature.* 389:785–786.

Hatada, I., H. Ohashi, Y. Fukushima, Y. Kaneko, M. Inoue, Y. Komoto, A. Okada, S. Ohishi, A. Nabetani, H. Morisaki, et al. 1996. An imprinted gene p57KIP2 is mutated in Beckwith-Wiedemann Syndrome. *Nat. Genet.* 14: 171–173.

Hughes-Benzie, R.M., G. Pilia, J.Y. Xuan, A.G.W. Hunter, E. Chen, M. Golabi, J.A. Hurst, J. Kobori, K. Marymee, R.A. Pagon, et al. 1996. Simpson-Golabi-Behmel Syndrome: genotype/phenotype analysis of 18 affected males from 7 unrelated families. *Am. J. Med. Genet.* 66:227–234.

Jackson, S.M., H. Nakato, M. Sugiura, A. Jannuzi, R. Oakes, V. Kaluza, C. Golden, and S.B. Selleck. 1997. *dally*, a *Drosophila* glypican, controls cellular responses to the TGF-beta-related morphogen Dpp. *Development.* 124: 4113–4120.

Jacobson, M.D., M. Weil, and M.C. Raff. 1997. Programmed cell death in animal development. *Cell.* 88:347–354.

Kleef, J., T. Ishiwata, A. Kumbasar, H. Friess, M.W. Buchler, A.D. Lander, and M. Korc. 1998. The cell surface heparan sulfate proteoglycan glypican-1 regulates growth factor in pancreatic carcinoma cells and is overexpressed in human pancreatic cancer. *J. Clin. Invest.* 102:1662–1673.

Lau, M.M., C.E. Stewart, Z. Liu, H. Bhatt, P. Rotwein, and C.L. Stewart. 1994. Loss of the imprinted IGF2/cation-independent mannose 6-phosphate receptor results in fetal overgrowth and perinatal lethality. *Genes Dev.* 8:2953–2963.

Lee, M.P., M.R. DeBaun, K. Mitsuya, H.L. Galonek, S. Brandenburg, M. Oshimura, and A.P. Feinberg. 1999. Loss of imprinting of a paternally expressed transcript, with antisense orientation to K_vLqt1, occurs frequently in Beckwith-Wiedemann syndrome and is independent of insulin-like growth factor II imprinting. *Proc. Natl. Acad. Sci. USA.* 96:5203–5208.

Leighton, P.A., R.S. Ingram, J. Eggenschwiler, A. Efstratiadis, and S.M. Tilghman. 1995. Disruption of imprinting caused by deletion of the H19 gene region in mice. *Nature.* 375:34–39.

Lindsay, S., H. Ireland, O. O'Brien, J. Clayton-Smith, J.A. Hurst, J. Mann, T. Cole, J. Sampson, S. Slaney, D. Schlessinger, et al. 1997. Large scale deletions in the GPC3 gene may account for a minority of cases of Simpson-Golabi-Behmel syndrome. *J. Med. Genet.* 34:480–483.

Ludwig, T., J. Eggenschwiler, P. Fisher, A.J. D'Ercole, M.L. Davenport, and A. Efstratiadis. 1996. Mouse mutants lacking the type 2 IGF receptor (IGF2R) are rescued from perinatal lethality in Igf2 and Igf1r null backgrounds. *Dev. Biol.* 177:517–535.

Nakato, H., T.A. Futch, and S.B. Selleck. 1995. The division abnormally delayed (*dally*) gene: a putative integral membrane proteoglycan required for cell division patterning during postembryonic development of the nervous system in *Drosophila*. *Development.* 121:3687–3702.

Neri, G., R. Marini, M. Cappa, P. Borrelli, and J.M. Opitz. 1988. Simpson-Golabi-Behmel syndrome: an X-linked encephalo-tropho-schisis syndrome. *Am. J. Med. Genet.* 30:287–299.

Neri, G., F. Gurrieri, G. Zanni, and A. Lin. 1998. Clinical and molecular aspects of the Simpson-Golabi-Behmel syndrome. *Am. J. Med. Genet.* 79:279–283.

Orstavik, R.E., N. Tommerup, K. Eiklid, and K.H. Orstavik. 1995. Non-random X chromosome inactivation in an affected twin in a monozygotic twin pair discordant for Wiedemann-Beckwith syndrome. *Am. J. Med. Genet.* 56:210–214.

Pellegrini, M., G. Pilia, S. Pantano, F. Lucchini, M. Uda, M. Fumi, A. Cao, D. Schlessinger, and A. Forabosco. 1998. Gpc3 expression correlates with the phenotype of the Simpson-Golabi-Behmel syndrome. *Dev. Dyn.* 213:431–439.

Pilia, G., R.M. Hughes-Benzie, A. MacKenzie, P. Baybayan, E.Y. Chen, R. Huber, G. Neri, A. Cao, A. Forabosco, and D. Schlessinger. 1996. Mutations in GPC3, a glypican gene, cause the Simpson-Golabi-Behmel overgrowth syndrome. *Nat. Genet.* 12:241–247.

Saunders, S., S. Paine-Saunders, and A.D. Lander. 1997. Expression of the cell surface proteoglycan glypican-5 is developmentally regulated in kidney, limb, and brain. *Dev. Biol.* 190:78–93.

Song, H.H., W. Shi, and J. Filmus. 1997. OCI-5/rat glypican-3 binds to fibroblast growth factor-2 but not to insulin-like growth factor-2. *J. Biol. Chem.* 272: 7574–7577.

Sorokin, L., and P. Ekblom. 1992. Development of tubular and glomerular cells of the kidney. *Kidney Int.* 41:657–664.

Steinfeld, R., H. Van Den Berghe, and G. David. 1996. Stimulation of fibroblast growth factor receptor-1 occupancy and signaling by cell surface-associated syndecans and glypican. *J. Cell Biol.* 133:405–416.

Stipp, C.S., E.D. Litwack, and A.D. Lander. 1994. Cerebroglycan: an integral membrane heparan sulfate proteoglycan that is unique to the developing nervous system and expressed specifically during neuronal differentiation. *J. Cell Biol.* 124:149–160.

Sun, F.L., W.L. Dean, G. Kelsey, N.D. Allen, and W. Raik. 1997. Transactivation of Igf2 in a mouse model of Beckwith-Wiedemann syndrome. *Nature.* 389:809–815.

Vainio, S., and S. Muller. 1997. Inductive tissue interactions, cell signaling, and the control of kidney organogenesis. *Cell.* 90:975–978.

Veugelers, M., J. Vermeesch, G. Reekmans, R. Steinfeld, P. Marynen, and G. David. 1997. Characterization of glypican-5 and chromosomal localization of human GPC5, a new member of the glypican gene family. *Genomics.* 40:24–30.

Wang, Z.Q., M.R. Fung, D.P. Barlow, and E.F. Wagner. 1994. Regulation of embryonic growth and lysosomal targeting by the imprinted Igf2/Mpr gene. *Nature.* 372:464–467.

Watanabe, K., H. Yamada, and Y. Yamaguchi. 1995. K-glypican: a novel GPI-linked heparan sulfate proteoglycan that is highly expressed in developing brain and kidney. *J. Cell Biol.* 130:1207–1218.

Weksberg, R., and J.A. Squire. 1996. Molecular biology of Beckwith-Wiedemann syndrome. *Med. Pediatr. Oncol.* 27:462–469.

Weksberg, R., J.A. Squire, and D.M. Templeton. 1996. Glypicans: a growing trend. *Nat. Genet.* 12:225–227.

Weng, E.Y., G.R. Mortier, and J.M. Graham. 1995. Beckwith-Wiedemann syndrome. *Clin. Pediatr.* 34:317–326.

Woolf, A.S., and C.M. Cale. 1997. Roles of growth factors in renal development. *Curr. Opin. Nephrol. Hypertens.* 6:10–14.

Yan, Y., J. Frisen, M.H. Lee, J. Massague, and M. Barbacid. 1997. Ablation of the CDK inhibitor $p57^{Kip2}$ results in increased apoptosis and delayed differentiation during mouse development. *Genes Dev.* 11:973–983.

Zhang, P., N.J. Liegeois, C. Wong, M. Finegold, H. Hou, J.C. Thompson, A. Silverman, J.W. Harper, R.A. DePinho, and S.J. Elledge. 1997. Altered cell differentiation and proliferation in mice lacking $p57^{KIP2}$ indicates a role in Beckwith-Wiedemann syndrome. *Nature.* 387:151–158.